PREPRINT UCRL-

Lawrence Livermore Laboratory

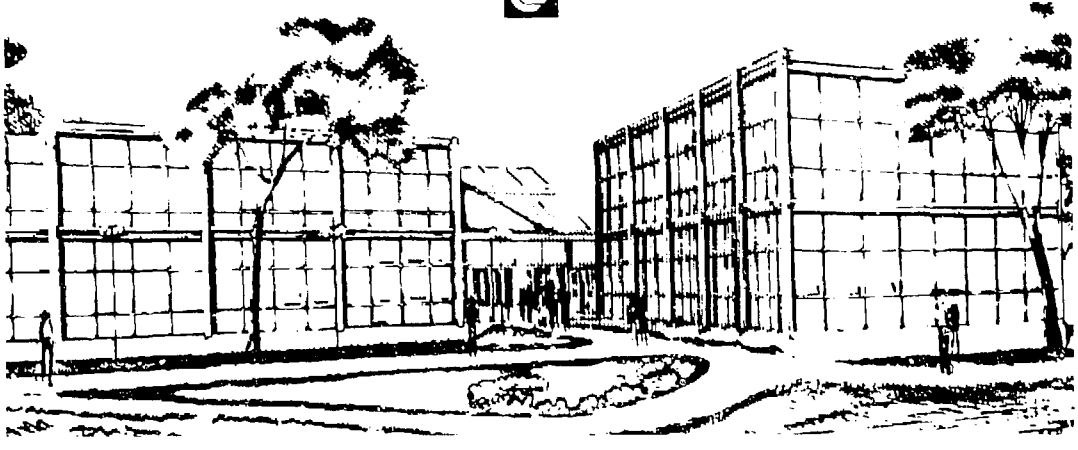

STRESS-RUPTURE LIFETIMES OF ORGANIC FIBER-EPOXY STRANDS AND PRESSURE VESSELS*

H. T. Hahn,** I. L. Chiu, and T. L. Gates

Lawrence Livermore Laboratory, University of California

Livermore, California 94550

ABSTRACT

To understand the long-term behavior of filament-wound pressure vessels, we tested Kevlar 49/epoxy strands in stress-rupture for more than a year. Because the strands are the smallest structural unit in filament winding, their behavior directly controls the performance of vessels.

Five different stress levels were studied: 86, 80, 74, 68, and 50% of the mean ultimate tensile strength (UTS). At each stress level, approximately one-hundred strands were hung in a room maintained at 22 to 24°C and below 20% relative humidity. Failure times were automatically recorded by a data acquisition system.

Lifetimes were analyzed statistically using a two-parameter Weibull distribution. The maximum-likelihood method was used to estimate the parameters. The shape parameter, which is a measure of scatter and failure-rate change, increased with decreasing stress level. In other words,

*This work was performed under the auspices of the U.S. Department of Energy by Lawrence Livermore Laboratory under contract No. W-7405-Eng-48.

**Present address: Department of Mechanical Engineering, Washington University, St. Louis, MO 63130.

less scatter and increasing failure rates were observed at lower stresses. There was no sign of an endurance limit down to 68% UTS. At 50% UTS no failure had yet occurred after 9000 h.

The strand data were compared with data on lifetimes of pressure vessels wound with the same fiber and epoxy. The strands had slightly longer characteristic lifetimes, except at 86% UTS, and slightly less scatter, except at 68% UTS.

The results of this study indicate that strands can provide valuable information about the long-term performance of filament-wound pressure vessels. Strands are much cheaper to fabricate and to test. Thus, where a high reliability is required, strands can provide data at the required confidence level.

INTRODUCTION

For a reliable and efficient application of composites, or any material for that matter, a comprehensive knowledge of their behavior under various loading environments is required. Especially in applications where long-term sustained loading is expected, stress-rupture behavior is very important.

In the present study, we have chosen composite strands to generate lifetime data under sustained tensile loading. Strand specimens offer several advantages over coupon specimens. First of all, they are very cost-effective because not much material is needed and the strands can be easily fabricated by filament winding. Second, because of much lower failure loads, they are easier to test than coupon specimens. Thus there is less likelihood of tab debonding, which is a major concern especially in long-term tests. Finally, because of small dimensions, the use of strand specimens can reduce preconditioning time considerably, which is important where environmental effects are involved. One obvious disadvantage, of course, is that they are not amenable to types of loading other than tension in the fiber direction.

In filament winding, the smallest building unit is a composite strand. Therefore, the next question addressed in the present paper is, How do strand properties translate into the behavior of filament-wound structures? In particular, we compare lifetimes of strands with those of pressure vessels.

Stress-rupture of composite strands has been extensively studied by Chiao et al. [1-5]. Material systems chosen were S-glass/epoxy [1], beryllium

wire/epoxy [2], organic fiber/epoxy [3], and graphite/epoxy [4]. Further updated results are summarized in [5]. The effect of elevated temperature on stress-rupture behavior of Kevlar 49/epoxy* can be found in [6].

In the present study, we have chosen Kevlar 49/epoxy composite because of its light weight and high tensile strength and also because the same material system was used in our recent study of stress-rupture of pressure vessels [7].

EXPERIMENTAL PROCEDURE

The fiber used was single-end, 380-denier, Kevlar 49 without sizing. Fiber strands were impregnated with an epoxy system, Dow Chemical DER 332/Jefferson Chemical Jeffamine T 403 (100/45 parts by weight), and were wound on racks, using a filament-winding machine. After curing for 24 h at 25°C plus 16 h at 85°C, the strands were cut from the racks and stored in a light-tight box. The resulting fiber-volume content ranged from 62 to 70% (average 67%). In strands, the average net cross-sectional area of the fiber was 2.988×10^{-2} mm^2.

Before mechanical testing, aluminum tabs were bonded to ends of strands, using a room-temperature curable adhesive. The gage length of each strand specimen was 25.4 cm.

All static tensile tests were carried out on a universal testing machine at a strain rate of 5%/min. The load-displacement relations were linear to failure. Failure loads were converted to fiber strengths using the net cross-sectional area of the fiber.

*Reference to a company or product name does not imply approval or recommendation of the product by the University of California or the U.S. Department of Energy to the exclusion of others that may be suitable.

Stress-rupture tests were performed on dead-weight loading stations. More than 400 strands were put on test concurrently. When a strand failed, the weight dropped onto an electrical switch, which then sent a signal to a data acquisition system. Thus, failure times were automatically recorded and stored in the computer memory.

The stress-rupture stations were in a controlled room where ambient temperature was maintained between 22 and 24^{o}C and relative humidity was 10%, with extremes of 6 and 20% on rare occasions.

RESULTS AND DISCUSSION

Static Strength

A total of 50 strand specimens were tested to determine the static-strength distribution. The average fiber strength was 3.237 GPa, with a coefficient of variation of 4.8%. The strength data were also analyzed by using a two-parameter Weibull distribution of the form

$$R_s(X) = \exp\left[-\left(\frac{X}{X_o}\right)^{\alpha_s}\right]. \qquad (1)$$

Here $R_s(X)$ is the probability of survival at X (i.e., of strength being greater than or equal to X) and $R_s(\ )$ hereafter will be called the strength distribution.

Experimentally, median ranks were used for $R_s(X)$. Suppose X_i is the ith strength in an ordered sample of n strengths. In the present case, n = 50. The probability of survival $R_s(X_i)$ at X_i is given by

$$R_s(X_i) = 1 - \frac{i - 0.3}{n + 0.4} \ . \tag{2}$$

The parameters α_s and X_o were determined by using the method of maximum likelihood [8],

$$\alpha_s = 25.92, \qquad X_o = 3.307 \text{ GPa} \ . \tag{3}$$

The experimental data and Eq. (1) are shown graphically in Fig. 1.

According to Eq. (1), the average strength $\bar{X}$ and the coefficient of variation (C.V.), respectively, are given by

$$\bar{X} = X_o \Gamma(1 + 1/\alpha_s) \ , \tag{4}$$

$$\text{C.V.} = \left[\Gamma(1 + 2/\alpha_s)/\Gamma^2(1 + 1/\alpha_s) - 1\right]^{1/2} \ , \tag{5}$$

where $\Gamma()$ is the gamma function. In conjunction with Eq. (3), Eqs. (4) and (5) lead to

$$\bar{X} = 3.238 \text{ GPa}, \qquad \text{C.V.} = 4.8\% \ . \tag{6}$$

These values agree very well with those calculated directly from the experimental data. The foregoing average fiber strength determined from strand tests is slightly higher than that obtained [9] from composite coupon tests (3.083 GPa), where the fiber strength is the composite strength divided by the fiber volume-fraction.

Stress Rupture

A summary of all stress-rupture tests is given in Table 1. Tests were complete at 86% of the average ultimate tensile strength (UTS), but they were still continuing at the other stress levels. No failure had occurred after 9000 h at 50% UTS. Where tests were not complete, the last failure times are also shown.

The lifetime data were analyzed again by using a two-parameter Weibull distribution of the form

$$R_\ell(t) = \exp\left[-\left(\frac{t}{t_o}\right)^{\alpha_\ell}\right], \tag{7}$$

where $R_\ell(t)$ is the probability of surviving time t and t_o is the characteristic lifetime. There is a question as to the plausibility of Eq. (7) when the applied stress is comparable to UTS [10]. At 86% UTS, the probability of static failure (i.e., the probability of a specimen failure before reaching the intended stress level) is calculated from Eq. (1) to be only 1.15%. Therefore, a two-parameter Weibull distribution, Eq. (7), is sufficient to describe lifetime distributions at stresses up to 86% UTS for the present material system. Again, the method of maximum likelihood was used to determine α_ℓ and t_o for both complete and censored data. In the case of censored data, the "last failure times" in Table 1 were used in the analyses. The results are listed in Table 1.

Lifetime distribution at each stress level is shown in Fig. 2. The solid curves represent Eq. (7) and the broken curves are for pressure vessels (discussed in following section). On the whole, Eq. (7) describes the experimental data fairly well. Figure 2b-d shows the censored nature of the

data. For Fig. 2b,c, we can reasonably expect subsequent failures to follow the curves. Because the curve in Fig. 2d is based on only three failures, the probability is high that the distribution will change as more data become available.

Figure 3 pictorially shows the parameters of Table 1. Figure 3a shows the shape parameter increasing with decreasing stress level. Thus there is less scatter at lower stress levels (see Eq. (5)). The shape parameter also provides a clue to the underlying failure processes in the strands (discussed below).

One method of characterizing a failure process is to use the failure rate, which is the probability of a specimen failing within a unit time interval. Experimentally, it is determined as the ratio of the number of failures during a unit time interval to the number of surviving specimens at a given instant. Since the lifetime distribution is given by Eq. (7), the failure rate (cf. Ref. 11) is as follows:

$$\text{Failure Rate} = \frac{-dR_\ell/dt}{R_\ell} = \frac{1}{t_o}\left(\frac{t}{t_o}\right)^{\alpha_\ell - 1} . \tag{8}$$

Thus one has either an increasing, a constant, or a decreasing failure rate, depending on whether α_ℓ is greater than, equal to, or smaller than unity.

Failure rates at different stress levels are shown in Fig. 4. These rates were determined from Eq. (8) using the shape parameters listed in Table 1. At 86% UTS, a decreasing failure rate characterizes the failure process; at the other stress levels, increasing failure rates are observed. Note that a decreasing failure rate indicates a failure process dominated by initial defects, and an increasing failure rate is a manifestation of a wear-out type of failure process.

Recently, a possible physical mechanism was suggested to explain the observed change of failure process with stress level [12]. Briefly, two failure mechanisms compete when a unidirectional composite is subjected to a tensile load in the fiber direction: the first mechanism is the normal crack-propagation mode, as in homogeneous brittle materials; the second is the parallel crack-propagation mode, an extreme example being observed in failure of dry fiber bundles. When the applied stress is high, the normal crack-propagation mode prevails initially. However, this gradually changes to the parallel crack-propagation mode as matrix and interface fail in the fiber direction. Because the former is associated with a higher probability of failure and the latter with a lower one, the failure rate decreases with time. When the applied stress is lower, however, the parallel crack-propagation mode dominates; there is no change of failure mode. Therefore, the composite failure is mostly because of stress-rupture of fibers with little stress concentration caused by broken fibers, and hence a wear-out type of failure process prevails.

A relation between the normalized applied stress and characteristic logarithmic lifetime is shown in Fig. 3b. Most commonly used equations to describe such relations are the power law and exponential law. When the data at 86% UTS are excluded, the power law is expected to work better. However, when all the data are included, the exponential law seems more appropriate. More definitive conclusions can be drawn when data at 50% UTS become available.

Because structural applications are based on earlier failures rather than on average or characteristic lifetimes, and also in order to appreciate scatter, we plotted in Fig. 5 lifetimes corresponding to R_ℓ = 0.99, 0.50 and 0.01. Equation (7) was used together with the parameters of Table 1. For a sample size of 100, for example, the left-hand curve indicates lifetimes for the first failure, and the right-hand curve shows when all samples but one

will fail. The middle curve indicates failure of half the samples. With horizontal shifts, all three curves are similar to the characteristic lifetime curve shown in Fig. 3b.

COMPARISON WITH PRESSURE VESSELS

To illustrate how strand behavior translates into behavior of filament-wound parts, we compare the data for strands with those for spherical pressure vessels. These vessels were wound with the same Kevlar 49/epoxy over aluminum liners. Structural details of these vessels are reported in Ref. 13. Basically, the aluminum liner has an outside radius of 57.2 mm and is 1-mm thick. The composite wall is 1.1-mm thick, quasi-isotropic, and has 65 vol% fibers.

The average burst pressure of vessels reported in Ref. 13 is 34.49 MPa. To compare the in situ fiber strength in vessels with that in strands, we first convert the burst pressure to a composite stress σ, assuming that a uniform state of stress exists in the composite skin and that the load sharing of the aluminum liner is negligible. From the spherical geometry of vessels, σ is found to be

$$\sigma = 914 \text{ MPa} . \tag{9}$$

Now, the strain ε under a biaxial stress σ becomes

$$\varepsilon = \frac{\sigma}{E} (1 - \nu) , \tag{10}$$

where E and ν are Young's modulus and Poisson's ratio, respectively, of the composite skin. Note that Eq. (10) presumes a linear stress-strain relation to failure. The elastic constants E and ν calculated in Ref. 13 are

$$E = 35.8 \text{ GPa}, \qquad \nu = 0.27 \ . \tag{11}$$

Substituting the values of Eq. (11) into Eq. (10) yields the composite failure strain $\varepsilon = 1.85\%$, which is very close to the actually observed failure strain.

Once the composite failure strain is known, the in situ fiber strength σ_f that corresponds to the average burst pressure is given by

$$\sigma_f = E_f \varepsilon = \frac{E_L (1 - \nu)}{V_f E} \sigma \ , \tag{12}$$

where the fiber modulus E_f has been estimated to be equal to the composite longitudinal modulus divided by the fiber volume fraction V_f. Noting that $E_L = 89.4$ GPa [13] and that $V_f = 0.65$ for the vessels studied, we finally determine the in situ fiber strength to be

$$\sigma_f = 2.544 \text{ GPa} \ . \tag{13}$$

The fiber strength in vessels is thus ~20% lower than that in strands.

The foregoing difference in fiber strength can be explained by the failure mode of vessels. All vessels failed along the weld lines between the aluminum liner and the bosses. Therefore, the stress concentration is believed to be responsible for the (average) in situ fiber strength in vessels being lower than that in strands.

However, the vessels exhibited less scatter in strength; the coefficient of variation was 3.7% for vessels as compared to 4.8% for strands. It is interesting that more uniformity of strength is possible in vessels.

Lifetime data of these vessels, as well as their analyses based on the Bayes methods, have been reported by Barlow, Toland, and Freeman [14]. In the present paper, however, we only use the maximum likelihood estimates of σ_ℓ and t_o. The results are summarized in Table 2. The lifetime distributions for vessels and strands are compared in Fig. 2a-d.

At 86% UTS, strand lifetimes are comparable to vessel lifetimes initially (see Fig. 2a). Later, however, vessel lifetimes begin to be longer. At the remaining stress levels (Fig. 2b-d), strands survive vessels, the difference being much smaller at 74% UTS than at 80 or 68% UTS. It should be noted, however, that the strand data at 68% are too few to allow any definitive conclusions.

In Fig. 3 the lifetime distribution parameters of vessels and strands are graphically compared. At every stress level tested except 68% UTS, the shape parameters (Fig. 3a) are slightly larger for strands than for vessels. The shape parameters increase with decreasing stress level. Except at 86% UTS, strands have longer characteristic lifetimes than vessels (Fig. 3b). Without the strand data at 86% UTS, the average slopes of stress-logarithmic lifetime curves for strands and vessels are almost equal.

For strands and vessels, lifetime data at three reliability levels are compared in Fig. 5. At the 0.99 reliability level (i.e., $R_\ell = 0.99$), strands survive vessels. As the reliability level decreases, the superiority of strands over vessels becomes mixed.

In Refs. 12 and 14, the same vessel data were compared with those of PRD-49-III/ERL 2258-ZZL 0820 strands. (Note that PRD-49-III is a preproduction version of Kevlar 49 fiber). These earlier strands exhibited shorter lifetimes than did vessels, except at $R_\ell = 0.99$ where the lifetimes were comparable [12]. Thus, on the average, the vessel lifetimes fall in between those of the present strands and of the earlier strands.

Major differences in the materials used and in the test procedure could account for the diverse results obtained for the present as opposed to the earlier strands. First, as mentioned earlier, the PRD-49-III fiber in the earlier strands was a preproduction version of the present Kevlar 49. Second, the epoxy system used in the present strands is DER 332-T 403, whereas it was ERL 2258-ZZL 0820 in the earlier strands. The strength of the latter epoxy system is about 50% higher than that of the former system, while the moduli are comparable [15, 16]. Finally, the test environment for the present strands was controlled better than for the earlier strands, the major difference being that the earlier strands were exposed to fluorescent lights during stress-rupture tests while the present strands were not. Any one or combination of these differences may lead to the observed discrepancy in stress-rupture behavior of the two types of strands. It is interesting, however, that the static strengths were comparable [17]. A further discussion of this subject can be found in Ref. 17.

CONCLUSIONS

We have presented preliminary stress-rupture lifetime data for Kevlar 49/epoxy (DER 332-T 403) strands and compared them with lifetime data of spherical pressure vessels wound with the same fiber and epoxy. The following conclusions are based on a two-parameter Weibull-distribution analysis of the data.

Strands

- Static strength distribution is represented by a shape parameter of 25.92 and a characteristic strength of 3.307 GPa.

- The shape parameter for lifetime distribution increases from below unity to above unity as the applied stress decreases from 86 to 68% UTS. The time-dependent failure process at 86% UTS is characterized by a decreasing failure rate, whereas an increasing failure rate is observed at 80, 74 and 68% UTS.

- There is no sign of an endurance limit down to 68% UTS. At 50% UTS, none of the 96 strands had failed after 9000 h.

Comparison With Vessels

- The nominal in-situ fiber strength for strands is higher than for fiber-wound vessels. The lower fiber strength for vessels is believed to result from the stress concentration along the weld lines in the aluminum liner. However, slightly less scatter in strength measurements is observed for the vessels.

- The lifetime shape parameter for strands is slightly larger than that for vessels, indicating less scatter for strands, except at 68% UTS.

- The strands enjoy longer characteristic lifetimes than the vessels, except at 86% UTS.

- On the whole, lifetimes of vessels are comparable to those of strands at the same fraction of the static strengths. Thus, additional confidence in the use of Kevlar 49/epoxy can be obtained from strand data, which are easier and more economical to generate than actual component data.

Stress-rupture tests are still continuing at lower stress levels. The lifetime distribution at 68% UTS is based on only three failures out of a total of 96 specimens, and, therefore, is subject to change as more data become available.

REFERENCES

1. T. T. Chiao, J. K. Lepper, N. W. Hetherington, and R. L. Moore, J. Compos. Mater. 6, 358 (1972).
2. T. T. Chiao, M. A. Hamstad, and E. S. Jessop, J. Compos. Mater. 8, 405 (1974).
3. T. T. Chiao, J. E. Wells, R. L. Moore, and M. A. Hamstad, in Composite Materials: Testing and Design (Third Conference), ASTM STP 546, 209 (1974).
4. R. L. Moore, M. A. Hamstad, and T. T. Chiao, Fukugo Zairyo (Composite Materials and Structures) 3, 19 (1974).
5. T. T. Chiao, C. C. Chiao, and R. J. Sherry, in Fracture Mechanics and Technology, Vol. 1, G. C. Sih and C. L. Chow, Eds. (Sijthoff and Noordhoff International Publishers, The Netherlands, 1977), p. 257.
6. C. C. Chiao, R. J. Sherry, and N. W. Hetherington, J. Compos. Mater. 11, 79 (1977).
7. R. E. Barlow, R. H. Toland, and T. Freeman, Stress-Rupture Life of Kevlar/Epoxy Spherical Pressure Vessels, Lawrence Livermore Laboratory, Report UCID-17755, Part 3 (1979).
8. A. C. Cohen, Technometrics 7, 579 (1965).
9. L. L. Clements and R. L. Moore, SAMPE Quarterly 9, 6 (1977).
10. H. T. Hahn, Composite Materials: Testing and Design (Fifth Conference), ASTM STP 674 (1979).
11. D. K. Lloyd and M. Lipow, Reliability: Management, Methods, and Mathematics (Prentice-Hall, Inc., Englewood Cliffs, New Jersey, 1962).
12. H. T. Hahn, "Proof Load Determination for Pressure Vessels Wound with Aramid Fiber," to be presented at the ASTM Symposium on Test Methods and Design Allowables, Dearborn, MI, Oct. 1979.

13. R. H. Toland, R. J. Sanchez, and D. Freeman, Stress-Rupture Life of Kevlar/Epoxy Spherical Pressure Vessels, Lawrence Livermore Laboratory, Report UCID-17755, Part 1 (1978).

14. R. E. Barlow, R. H. Toland, and T. Freeman, Stress-Rupture Life of Kevlar/Epoxy Spherical Pressure Vessels, Lawrence Livermore Laboratory, Report UCID-17755, Part 3 (1979).

15. T. T. Chiao and R. L. Moore, "A Room-Temperature-Curable Epoxy for Advanced Fiber Composites," in Proceedings of the SPI 29th Annual Technical Conference (1974), Section 16-B.

16. T. T. Chiao and L. P. Althouse, "Characterization of an Epoxy System for Filament Winding," in Proceedings of the Fourth National SAMPE Technical Conference (1972), 161.

17. H. T. Hahn and T. T. Chiao, "Long-Term Behavior of Composite Materials," in preparation.

YDB/ld

TABLE 1. Stress-rupture test status of strands.

Applied stress (% UTS)	Total specimens (No.)	Failures (No.)	Last failure time (h)	Shape parameter α_ℓ	Characteristic lifetime t_o (h)
86	94	94	--	0.766	4.731×10^1
80	101	69	3011	1.226	2.639×10^3
74	96	57	9253	1.339	9.763×10^3
68	95	3	8141	1.433	8.967×10^4
50	96	0	>9000	--	--

TABLE 2. Stress-rupture test status of vessels.

Applied pressure (% average burst pressure)	Total vessels (No.)	Failures (No.)	Last failure time (h)	Shape parameter α_ℓ	Characteristic lifetime t_o (h)
86	39	39	0.521	0.521	1.658×10^2
80	24	24	0.873	0.873	8.387×10^2
74	24	20	11727	1.107	7.445×10^3
68	21	7	16104	1.374	2.744×10^4
50	47	0	>17520	--	--

FIGURE CAPTIONS

FIG. 1. Static strength distribution of strands. The solid line represents Eq. (1).

FIG. 2. Lifetime distributions of strands and vessels: (a) at 86% UTS, (b) at 80% UTS, (c) at 74% UTS, and (d) at 70% UTS. The solid line and symbols are for strands and the dashed line is for vessels.

FIG. 3. Relations between applied stress and (a) shape parameter or (b) characteristic lifetime. Open symbols indicate censored data.

FIG. 4. Change of failure rate for strands. An increasing failure rate is observed at 86% UTS, whereas a decreasing failure rate is observed at the other stress levels.

FIG. 5. Stress-lifetime relations at three different reliabilities, R_ℓ = 0.99, 0.50, and 0.01. Strands enjoy longer lifetimes except at 86% UTS.

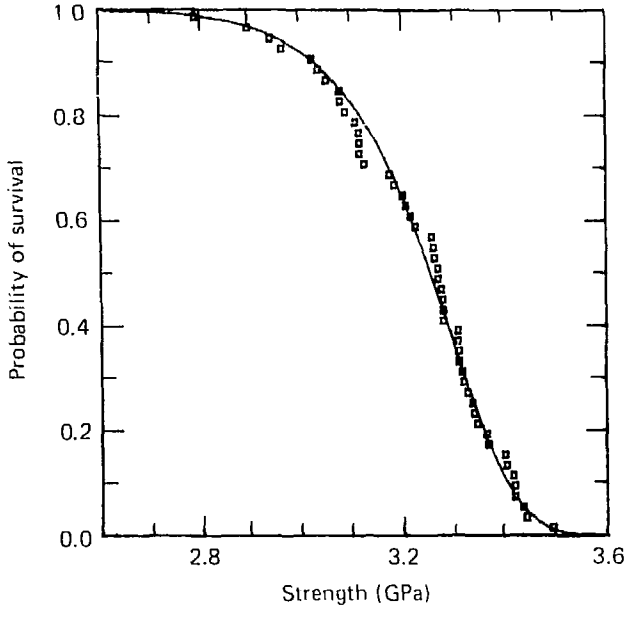
1.0
0.8
0.6
0.4
0.2
0.0
Probability of survival
2.8
3.2
3.6
Strength (GPa)

Hahn - Fig. 1

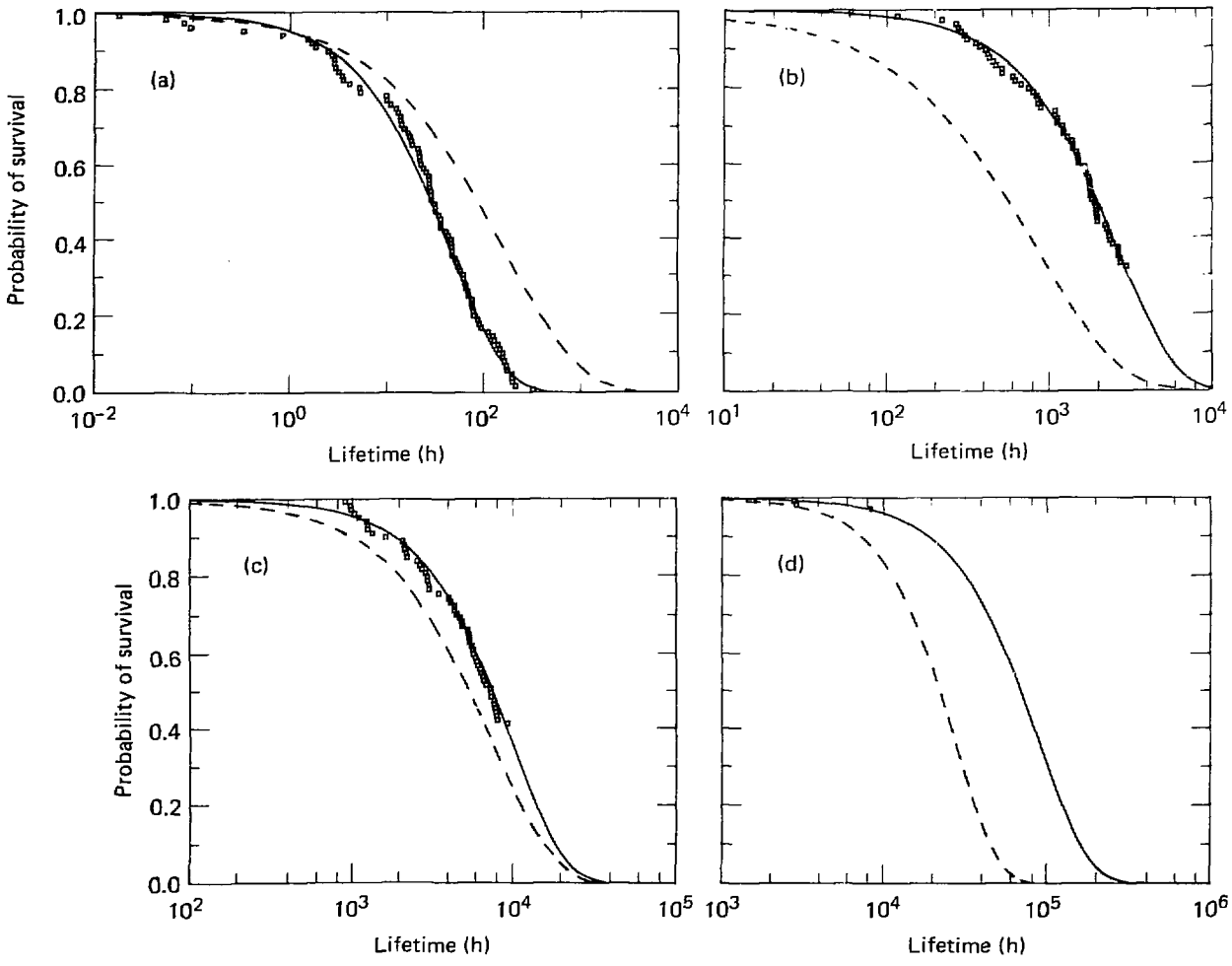
Probability of survival
1.0
0.8
0.6
0.4
0.2
0.0
(a)
10^{-2}
10^{0}
10^{2}
10^{4}
Lifetime (h)
(b)
10^{1}
10^{2}
10^{3}
10^{4}
Lifetime (h)
Probability of survival
(c)
10^{2}
10^{3}
10^{4}
10^{5}
Lifetime (h)
(d)
10^{3}
10^{4}
10^{5}
10^{6}
Lifetime (h)

Hahn - Fig. 2

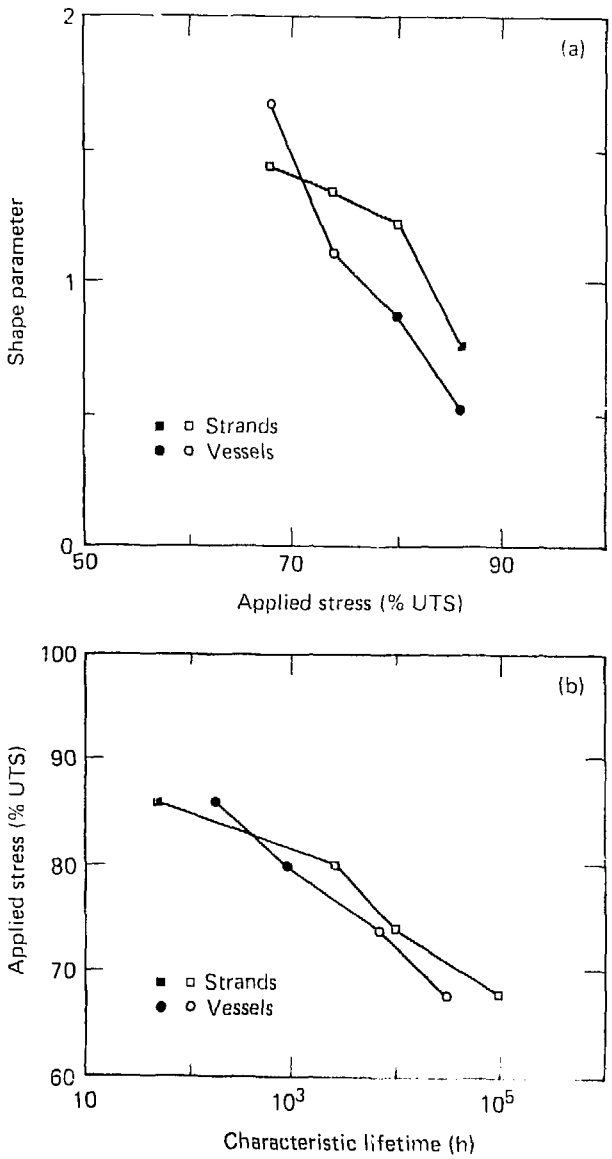
(a)
Shape parameter
2
1
0
50
70
90
Applied stress (% UTS)
Strands
Vessels
(b)
Applied stress (% UTS)
100
90
80
70
60
10
10^3
10^5
Characteristic lifetime (h)
Strands
Vessels

Hahn - Fig. 3

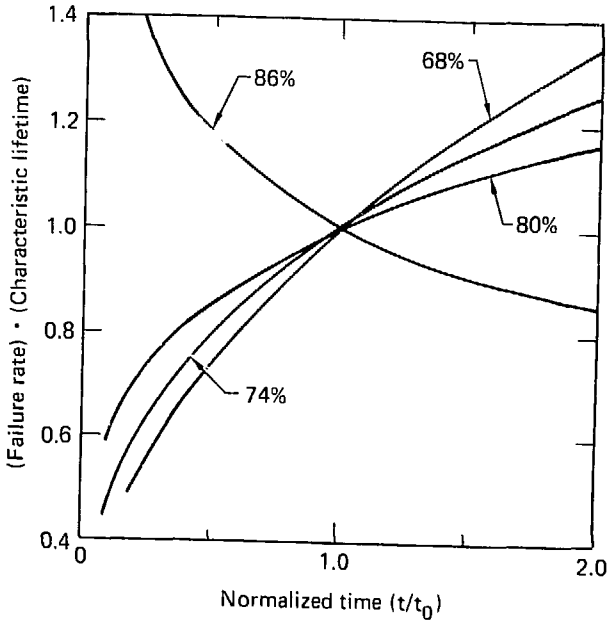
1.4
1.2
1.0
0.8
0.6
0.4
0
1.0
2.0
(Failure rate) • (Characteristic lifetime)
Normalized time (t/t0)
86%
68%
80%
74%

Hahn - Fig. 4

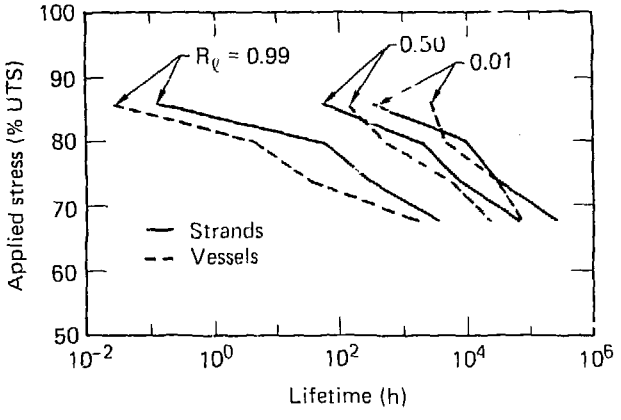
100
90
80
70
60
50
Applied stress (% UTS)
R_ℓ = 0.99
0.50
0.01
Strands
Vessels
10^{-2}
10^{0}
10^{2}
10^{4}
10^{6}
Lifetime (h)

Hahn - Fig. 5